Plasma Phys. Control. Fusion **54** (2012) 112001 (5pp) doi:10.1088/0741-3335/54/11/112001

BRIEF COMMUNICATION

Edge turbulence velocity changes with lithium coating on NSTX

B Cao[1], S J Zweben[2], D P Stotler[2], M Bell[2], A Diallo[2], S M Kaye[2] and B LeBlanc[2]

[1] Institute of Plasma Physics Chinese Academy of Sciences, Hefei 230031, People's Republic of China
[2] Princeton Plasma Physics Laboratory, PO Box 451, Princeton, NJ, 08540 USA

Received 24 July 2012, in final form 15 September 2012
Published 18 October 2012
Online at stacks.iop.org/PPCF/54/112001

Abstract
Lithium coating improves energy confinement and eliminates edge-localized modes in the National Spherical Torus Experiment (NSTX), but the mechanism of this improvement is not yet well understood. We used the gas-puff-imaging diagnostic on NSTX to measure the changes in edge turbulence which occurred during a scan with variable lithium wall coating, in order to help understand the reason for the confinement improvement with lithium. There was a small increase in the edge turbulence poloidal velocity and a decrease in the poloidal velocity fluctuation level with increased lithium. The possible effect of varying edge neutral density on turbulence damping was evaluated for these cases in NSTX.

(Some figures may appear in colour only in the online journal)

1. Introduction

Lithium coating is a very effective method for wall conditioning in tokamaks. It was recently used both on the National Spherical Torus Experiment (NSTX) and the Experimental Advanced Superconducting Tokamak (EAST), and both have achieved very good results; for example, the first H-mode plasma appeared after wall conditioning by lithium on EAST [1]. On NSTX lithium wall coating has been shown to reduce recycling, improve energy confinement, and suppress edge-localized modes (ELMs) [2–5]. The underlying cause of this improvement in confinement with increased lithium is not yet well understood in terms of the microscopic transport physics, although some decreases in edge turbulence with increased lithium were measured using reflectometry and high-k scattering [3]. This paper describes measurements made using the gas-puff-imaging(GPI) diagnostic of edge turbulence during a scan of lithium coating in NSTX, and analysis carried out in order to help determine if changes in edge turbulence velocity are correlated with the improvement in confinement. These measurements are made within ± 2 cm of the separatrix, so are somewhat farther out in radius than the profile and turbulence changes reported near $r/a = 0.8$ in [2, 3].

It is widely believed that the transition from low confinement (L-mode) to high confinement (H-mode) in tokamaks involves turbulence stabilization by shear flow [6]. Earlier theoretical and experimental work also suggested that charge-exchange (CX) collisions might have an important role in modifying the ion flow in the edge plasma where neutral concentration is high [7–12], and in affecting the L–H translation threshold power [13–18]. Thus because lithium coating reduces recycling, this should change the edge neutral density and CX collision rate, and so might cause a decrease in turbulence and improvement in confinement. This possible mechanism is evaluated in this paper using GPI measurements of edge turbulence, turbulence flow velocity and neutral density modeling to estimate the CX damping rate.

This paper is organized as follows: section 2 describes the parameters for the shots used in this lithium scan. The GPI data analysis techniques and results with varying lithium coatings are described in section 3, and an evaluation of the change exchange damping effects with varying lithium is in section 4. Finally, in section 5 we summarize and discuss the results.

2. Database for this analysis

The discharges used in this paper were all standard NSTX near-double-null, neutral beam heated, deuterium divertor plasmas taken on 21 October 2010. The main parameters of the eight shots used in this paper are shown in table 1. The GPI data for

Table 1. Shot list of database.

Shot	Start time (ms)	End time (ms)	P_{NBI} (MW)	W_{MHD} (J)	P_{loss} (MW)	$\tau_{E(MHD)}$ (s)	$H_{98(y,2)}$	n_e (10^{15} cm^{-2})	I_p (KA)	B (kG)	β_N	Edge pressure (10^{-5} Torr)	Li dep'n (mg)	Li accum (mg)
141307	480	490	3.8	1.37E + 05	4.2	0.032	0.893	7.5	700	4.43	4.45	5.82	22	1497
141309	480	490	4.8	1.60E + 05	5.2	0.031	0.837	7.8	700	4.43	4.90	6.76	22	1540
141319	530	540	3.9	1.42E + 05	4.0	0.035	0.877	7.9	650	4.43	4.87	4.7	90	2041
141320	530	540	4.0	1.42E + 05	4.0	0.035	0.952	8	650	4.43	4.98	4.66	90	2131
141321	530	540	3.9	1.41E + 05	4.8	0.029	0.809	7	650	4.43	4.27	5.42	89	2220
141322	530	540	4.0	1.48E + 05	4.2	0.035	1.02	8	650	4.43	5.02	4.8	151	2371
141324	530	540	2.9	1.26E + 05	2.8	0.045	1.22	6	650	4.43	4.96	3.1	246	2845
141326	530	540	2.9	1.57E + 05	2.9	0.054	1.33	5.6	650	4.43	5.62	3.06	314	3396

these eight shots were analyzed over a 10 ms period between the 'start' and 'end' times in this table, which were during the steady-state H-mode of these discharges during times without any ELMs. At these times the shots had a toroidal magnetic field 4.3 kG, plasma currents of 650–700 kA and neutral beam injection (NBI) powers of 2.9–4.8 MW. Note that the two shots with the highest lithium also had the lowest NBI power, in order to keep the normalized beta $\beta_N = \beta_T/(I/aB)$ constant at about 5.

The last two columns in table 1 show the lithium deposited just before this shot and the total lithium deposited during this day before this shot. The lithium deposited before each shot increased from about 20–300 mg over this sequence of eight shots. The maximum lithium ever deposited in between shots in NSTX was 900 mg in 2008 [2], i.e. about 3 times the lithium deposited in this paper; however, no GPI data were available from those shots in [2]. The shots in table 1 were a subset of the shots taken on the same run day used in [3] when GPI data were available and when there were no ELMs during the GPI measurements.

Figure 1 shows the variation of the some plasma parameters during the scan of table 1 during the GPI puffing time. Figure 1(*a*) shows the normalized beta β_N, which was approximately constant for these eight shots. Figures 1(*b*) shows the injected NBI power, in which there was a decrease for the two highest lithium coating shots in order to keep β_N constant. Figure 2(*c*) shows the $H_{98(y,2)}$ empirical thermal confinement scaling coefficient [19], which was generally increased with increasing lithium deposited, as observed previously [2–4]. This suggests that a slightly better energy confinement time was obtained with more lithium deposited before these shots (at constant β_N). Figure 1(*d*) shows the total lower divertor D_α emission, which indicates the recycling decreased for the highest lithium shots, as did the injected NBI power. Figure 1(*e*) shows the evolution of the edge pressure as measured by an ion gauge at vessel wall near outer midplane. The edge pressure also decreased with more lithium coating prior to the shot, implying fewer neutral particles in the outer midplane edge as a result of reduced outgassing and recycling from the wall, consistent with previous observations [4].

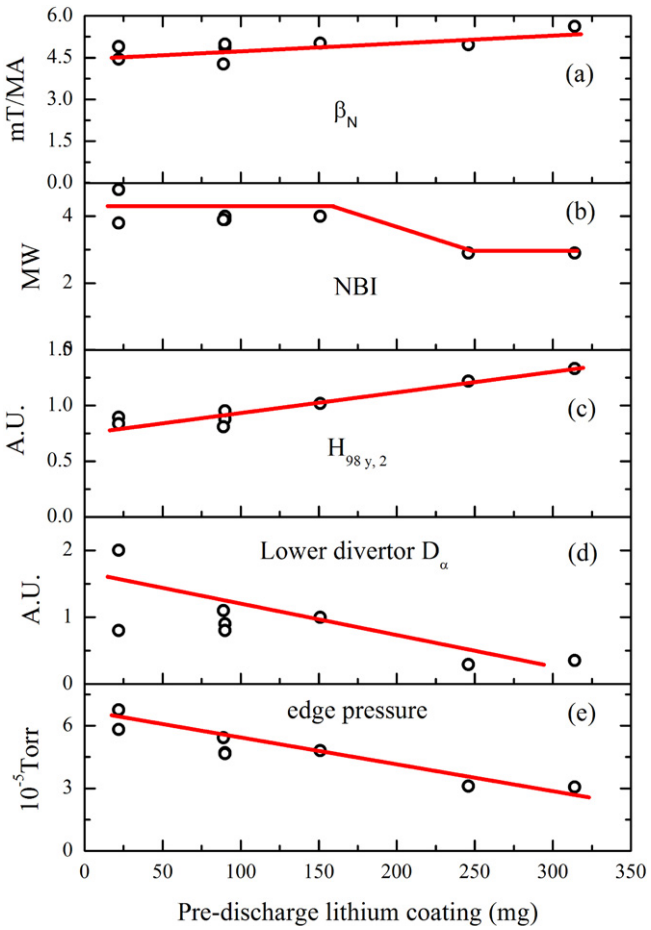

Figure 1. Main parameter changes with lithium: (*a*) shows the β_N, (*b*) shows the injected NBI power, (*c*) shows the empirical scaling coefficient $H_{98y,2}$, (*d*) shows the divertor D_α light and (*e*) shows the edge pressure. The red lines are linear fits of these points, except for (*b*).

3. GPI data analysis

A brief review of the GPI diagnostic on NSTX is included here, more details can be found in these papers [20, 21]. The GPI measurement on NSTX is a two-dimensional diagnostic of the edge turbulence near the outer midplane. A gas puffing manifold located at the outer wall provides a deuterium gas puff into the plasma, and the visible D_α emission from this gas cloud is then imaged by a fast camera. Since the turbulence is highly elongated along the magnetic field, the D_α light from GPI gas puff cloud was viewed along the local magnetic field to resolve the radial versus poloidal structure of turbulence.

The edge turbulence measured by GPI near the separatrix in this experiment had a typical radial correlation length of ~4–7 cm, a typical poloidal correlation length ~5–10 cm and

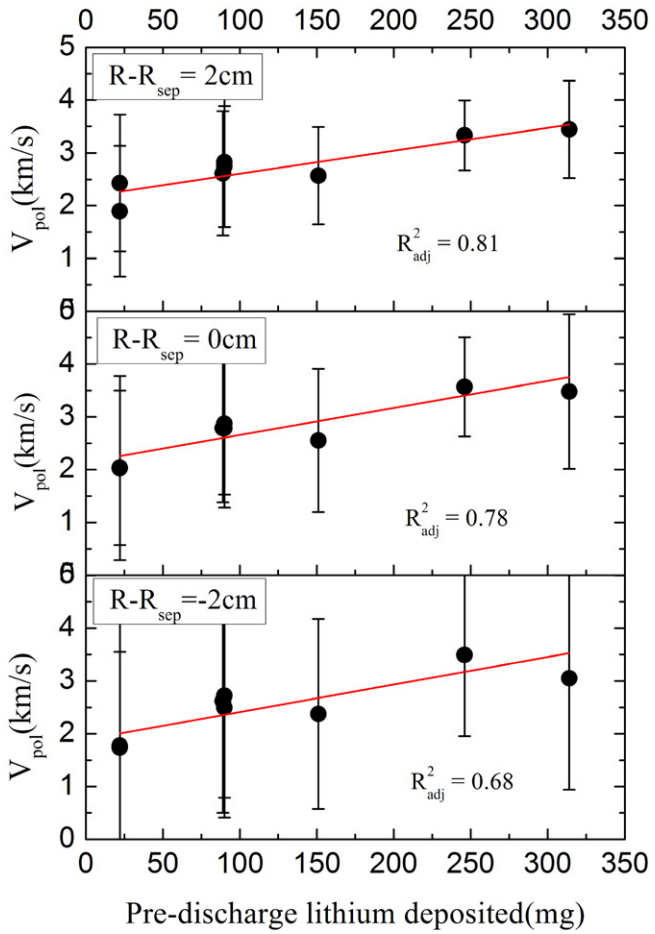

Figure 2. Poloidal turbulence velocities versus lithium at different radial locations ($R - R_{sep} = -2, 0, 2$ cm). The error bars are the RMS variations of V_{pol} at each point. The average poloidal velocity increases from $\sim$2 km s^{-1} to $\sim$3 km s^{-1} with more lithium for all radii. The quality of the fits is described by the adjusted R^2_{adj} values in each panel.

an autocorrelation time of $\sim$20–60 μs, which are similar to previous GPI measurements in NSTX [20, 21]. This is a much higher size scale than electron temperature gradient modes, but perhaps comparable to edge ion temperature gradient or microtearing instabilities.

To evaluate the poloidal flow speed of the turbulence, for every pixel for each frame during the 10 ms of interest we evaluated time delay of the peaks of the poloidal cross-correlation functions of nearby pixels as a function of poloidal separation, using a time averaging for each cross-correlation of $\pm$10 frames (i.e. over $\sim$25 μs), similar to the procedure in [21]. We then fit these time delays to obtain a local poloidal turbulence velocity for each pixel for each time, which results in a time-resolved poloidal velocity with a frequency response of $\sim$40 kHz. We then averaged these poloidal velocities over the poloidal range of the GPI data at each radius. Figure 2 shows the resulting average poloidal velocity as a function of the pre-discharge lithium level, along with the RMS fluctuation levels in the poloidal velocity shown as error bars. There is systematic trend for an increase in the poloidal velocity with more lithium, i.e. $V_{pol} = 2$–3 km s^{-1}, independent of radius over $R - R_{sep} = -2, 0$ and 2 cm. This velocity is in the electron

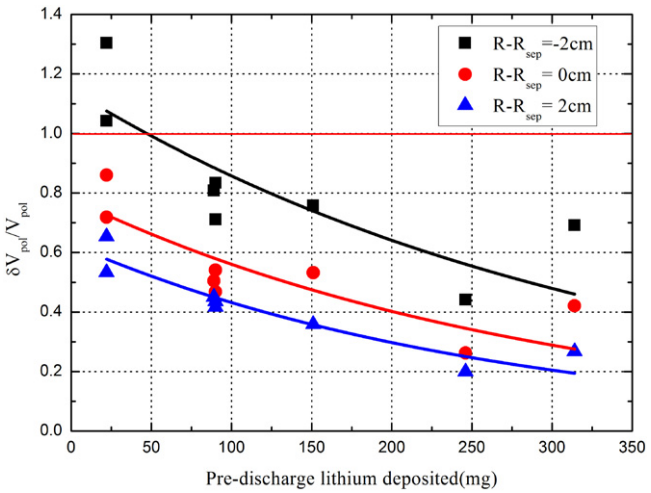

Figure 3. Fluctuating part of the poloidal velocity (δV_{pol}) divided the mean poloidal velocity (V_{pol}) at different radial locations versus the amount of lithium coating before shot. The $\delta V_{pol}/V_{pol}$ decreased with increased lithium coating.

diamagnetic drift direction. Although there is an unknown level of uncertainty in the evaluation of the separatrix position using the standard magnetic equilibrium fitting code EFIT (which may be up to $\sim$2 cm), we assume that this uncertainty does not depend on the amount of lithium, so the trend of increasing poloidal velocity with increased lithium should be fairly reliable. Note that the error bars are not experimental errors in the estimate of V_{pol}, but the time-dependent RMS fluctuation levels of V_{pol} estimated using this technique. Note that passive or active spectroscopic measurements of the carbon ion poloidal rotation on NSTX are not be directly related to these turbulence velocity measurements, since the turbulence is presumably affected by the main ion fluid $E \times B$ motion (see section 5).

Figure 3 shows the fluctuating part of poloidal velocity δV_{pol} divided the time-averaged poloidal velocity V_{pol} versus the amount of lithium coating before shot for the same data as in figure 2. The relative fluctuations in the turbulence poloidal velocity are decreasing by a factor of $\times$2–3 with increased lithium at each radius, in part from the increase in V_{pol} with increased lithium (figure 2). These fluctuations are in the range up to $\sim$40 kHz, and since they are averaged over the poloidal range of the GPI data, might be associated with 'zonal flows', similar to the analysis of GPI data for Alcator C-Mod [22].

4. Evaluation of CX versus lithium deposition

As mentioned in section 1, it is not yet clear why coating the wall surfaces with lithium should affect the plasma energy confinement time. One potential mechanism for this is that the lithium coating reduces the outgassing and recycling of deuterium from the wall, and this in turn reduces the neutral deuterium density in the plasma edge. The edge neutral density can in theory affect the $E \times B$ flow and flow shear in the edge, which can in principle affect the edge turbulence and its resulting transport. A correlation between increased energy confinement and decreased edge turbulence was described

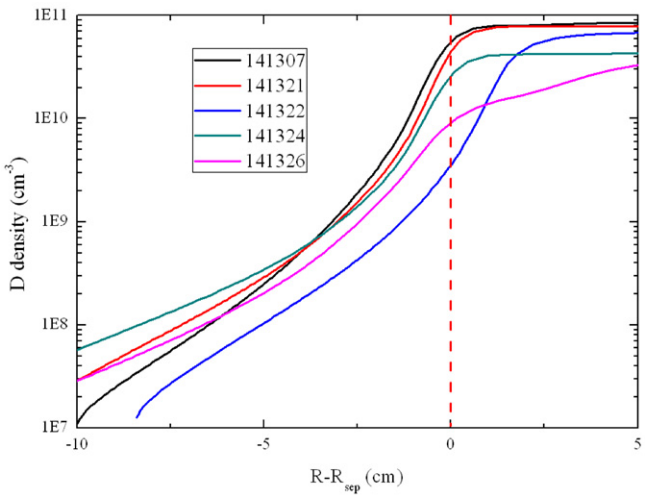

Figure 4. Edge neutral density profiles from neutral particle simulation codes of KN1D, using the plasma electron density and temperature profiles from Thomson Scattering diagnostic and the edge pressures from ion gauge shown in table 1. The lithium coating increased with shot number.

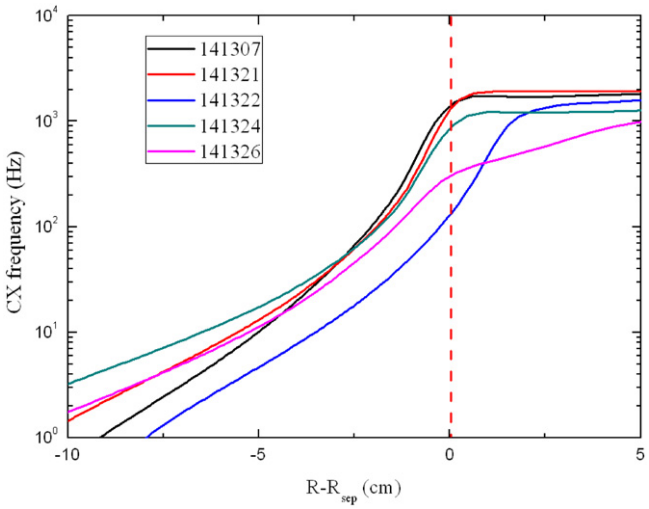

Figure 5. Ion CX collision frequency profiles from neutral particles simulation results with the same labels as for figure 4. The lithium coating increased with shot number.

previously in the context of lithium coating experiments on NSTX [3]. Previous work on DIII-D [13, 16, 17] and NSTX [18] also showed that the CX damping introduced by neutrals could play an important role in the L–H translation.

Here we evaluate the effect of CX collisions during the NSTX lithium scan described in this paper. Such collisions can introduce a damping of ion flow in both the parallel (along B) and poloidal directions [7–12], which could then potentially affect edge $E \times B$ flow and edge turbulence. Generic theoretical estimates [11] indicated that the modification of ion flow due to CX can be significant when the ratio of neutral density to electron density was $n_n/n_e > 10^{-3}$. Results from the 2D fluid turbulence simulation code SOLT also suggested that edge turbulence and radial transport decreased as the $E \times B$ flow damping parameter increased [23]. As mentioned in [24], the time-averaged transport coefficient has a maximum value when the mean $E \times B$ flow equals the oscillatory part of $E \times B$ flow. So it is possible that the increase in H factor with lithium as shown in figure 2 could be due to changes in either the mean or fluctuating $E \times B$ flow.

Figure 4 shows the simulated midplane neutral density profiles from a KN1D code analysis [25] using the plasma electron density and temperature profiles from Thomson scattering diagnostic and the edge pressures from the ion gauge measurements shown in table 1. The lithium coating increased with shot number. Figure 5 shows the CX damping rate for ions calculated from figure 4. In the radial range ± 2 cm around the separatrix where the turbulence was measured in figures 3 and 4, the neutral density and CX damping rate generally decreased with more lithium coating. This is qualitatively consistent with the expectation that the edge CX damping should decrease with increase lithium coating. An exception is shot #141322 in which the high edge density and temperature makes the neutral density decrease unusually low in the SOL. The uncertainty in these neutral profiles depends mainly on the uncertainty in the Thomson profiles since the CX cross-sections are well known.

5. Summary and discussion

This paper presented the results of GPI measurements in NSTX with increasing lithium coating. During the scan of lithium deposition for the eight shots in this database, we observed a slight increase in H factor (figure 2), which was also seen in previous lithium deposition scans on NSTX [2–4]. For the same scan we found with increasing pre-discharge lithium deposition a slight decreased edge pressure (figure 1) and a slight increase in the poloidal flow speed both inside and outside the EFIT separatrix (figure 2).

There is not yet an unique interpretation of these results in terms of edge turbulence physics. The observed increased poloidal flow of the turbulence could simply be due to the increase in the edge density gradient with increased lithium, which could cause the observed increase in the phase speed of the turbulence in the electron diamagnetic direction. The increased poloidal turbulence speed could also be affected by changes in the toroidal plasma rotation, which were not measured during this scan. There may be an increase in poloidal flow shear associated with the increase in poloidal turbulence rotation, but the magnitude of the local flow shear could not be evaluated accurately enough in these data set to show any systematic trend with lithium. In this sense the present results are similar to those discussed previously [2, 3], in which a correlation was observed between edge turbulence, lithium coating and the effects on confinement, but a causal relationship was not proven.

As discussed in section 1, one possible causal connection between the lithium wall coating and the plasma energy confinement time could be through the decrease in edge neutral density with increased lithium. Assuming that the global energy confinement time depends on the edge turbulence transport, if the edge neutral density reduced the edge turbulent transport, then it could also cause an increase in the global energy confinement time. One possible mechanism for the edge neutrals to affect the edge turbulence is through the CX collision, where a decrease in CX collision with increased

lithium could cause a viscosity and modification of the ion distribution function in the parallel flow and flow shear of the turbulence [7–11], according to [6].

Two new pieces of evidence for such a causal connection were described in this paper; namely, a slight increase in the mean poloidal flow speed with increasing lithium (figure 2), and a decrease in the relative poloidal flow fluctuations (figure 3). These point to a possible change in edge shear or zonal flow with increasing lithium. An attempt to directly evaluate the CX damping effect showed that the CX collision frequency in figure 5 was small compared with ion transit and edge turbulence frequency (about 10^4 Hz) inside the separatrix, but a quantitative evaluation of the effect of CX on the poloidal flow speed or shearing rate was not attempted. Note that [12] suggested that the CX damping can play a very important role in this region.

There were certainly limitations and uncertainties in the present data and analysis. The main limitations came from the relatively few shots available with GPI data for these NSTX lithium scans, and in particular the decrease in NBI power for the two shots with the highest lithium coating. Although this decrease in NBI power was done intentionally to keep the plasma beta constant, a previous study indicated that edge turbulence in NSTX was correlated with the NBI power [26]. Therefore the relative effects of NBI power and lithium coating on the edge turbulence could not be determined from this scan.

Further work on the confinement effects of lithium is needed to clarify the physical mechanisms involved. More systematic experiments are needed to separate the effects of lithium coating from the effects of varying NBI. More detailed measurements of the edge plasma flow velocity and velocity shear should be made and correlated with measurements of the edge particle and heat transport due to turbulence. Finally, direct measurements should be made of the neutral density profile at multiple poloidal locations, and the effects of CX neutral damping should be evaluated based on computational simulations of edge turbulence and transport.

Acknowledgments

The authors wish to thank B LaBombard of MIT and B Davis of PPPL for the help with KN1D, R J Maqueda for taking the GPI data used in this experiment, F Scotti of PPPL for the help with the calibration of the GPI camera, V Soukanovskii and F Scotti for divertor data and R J Maqueda, R Maingi, J M Canik and W X Wang for very helpful comments. One of us (Bin Cao) thanks the NSTX team for support during his visit to PPPL. This research was funded by the National Nature Science Foundation of China under Contract No 11021565 and US DOE Contract DE-AC02-09CH11466.

References

[1] Xu G X *et al* 2011 *Nucl. Fusion* **51** 072001
[2] Maingi R *et al* 2011 *Phys. Rev. Lett.* **107** 145004
[3] Canik J M *et al* 2011 *Phys. Plasmas* **18** 056118
[4] Maingi R *et al* 2012 *Nucl. Fusion* **52** 083001
[5] Boyle D P *et al* 2011 *Plasma Phys. Control. Fusion* **53** 105011
[6] Terry P W 2000 *Rev. Mod. Phys.* **72** 109
[7] Valanju P M, Calvin M D, Hazeltine R D and Solano E R 1992 *Phys. Fluids* B **4** 2675
[8] Catto P J, Helander P, Connor J W, and Hazeltine R D 1998 *Phys. Plasmas* **5** 3961
[9] Fulop T, Helander P and Catto P J 2002 *Phys. Rev. Lett.* **89** 22
[10] Fulop T, Catto P J and Helander P 1998 *Phys. Plasmas* **5** 3398
[11] Fulop T, Catto P J and Helander P 2001 *Phys. Plasmas* **8** 5214
[12] Xu G S *et al* 2011 *Plasma Sci. Technol.* **13** 397
[13] Mahdavi M A *et al* 1990 *J. Nucl. Mater.* **176–177** 32
[14] Owen L W *et al* 1998 *Plasma Phys. Control. Fusion* **40** 717–20
[15] Tsuchiya K *et al* 1996 *Plasma Phys. Control. Fusion* **38** 1295–9
[16] Carreras B A *et al* 1998 *Phys. Plasmas* **5** 2623
[17] Carreras B A, Diamond P H and Vetoulis G 1996 *Phys. Plasmas* **3** 4106
[18] Maingi R *et al* 2004 *Plasma Phys. Control. Fusion* **46** A305
[19] ITER Physics Basis 1999 *Nucl. Fusion* **39** 1295
[20] Maqueda R J *et al* 2003 *Rev. Sci. Instrum.* **74** 2020
[21] Zweben S J *et al* 2010 *Phys. Plasma* **17** 102502
[22] Zweben S J *et al* 2012 *Plasma Phys. Control. Fusion* **54** 025008
[23] Russell D A *et al* 2009 *Phys Plasmas* **16** 122304
[24] Maeyama S, Ishizawa A, Watanabe T H, Škorić M M, Nakajima N, Tsuji-Iio S and Tsutsui H 2010 *Plasma Phys.* **17** 062305
[25] LaBombard B 2001 KN1D: A 1-D Space, 2-D Velocity, kinetic transport algorithm for atomic and molecular hydrogen in an ionizing plasma, PSFC/RR-01-3 (MIT), also http://www.psfc.mit.edu/∼labombard/KN1D_Source_Info.html
[26] Maqueda R J *et al* 2011 *J. Nucl. Mater.* **415** S459